



**HAL**  
open science

## **A case report of changes in asymmetric colour use in paintings produced over 3 years post-stroke by a patient with spatial neglect.**

Gilles Rode, Eric Chabanat, Marine Lunven, Juliette Courtille, Patrice Revol, K T Reilly, Laure Pisella, Yves Rossetti

### **► To cite this version:**

Gilles Rode, Eric Chabanat, Marine Lunven, Juliette Courtille, Patrice Revol, et al.. A case report of changes in asymmetric colour use in paintings produced over 3 years post-stroke by a patient with spatial neglect.. *Communications Psychology*, 2025, 3 (52), <10.1038/s44271-025-00226-5>. <hal-04982175>

**HAL Id: hal-04982175**

**<https://hal.science/hal-04982175v1>**

Submitted on 13 Jun 2025

**HAL** is a multi-disciplinary open access archive for the deposit and dissemination of scientific research documents, whether they are published or not. The documents may come from teaching and research institutions in France or abroad, or from public or private research centers.

L'archive ouverte pluridisciplinaire **HAL**, est destinée au dépôt et à la diffusion de documents scientifiques de niveau recherche, publiés ou non, émanant des établissements d'enseignement et de recherche français ou étrangers, des laboratoires publics ou privés.



Distributed under a Creative Commons CC BY 4.0 - Attribution - International License



# A case report of changes in asymmetric colour use in paintings produced over 3 years post-stroke by a patient with spatial neglect



Gilles Rode <sup>1,2,6</sup> , Eric Chabanat <sup>1,6</sup>, Marine Lunven <sup>3</sup>, Juliette Courtille <sup>4</sup>, Patrice Revol <sup>1,2</sup>, Karen T. Reilly <sup>1</sup>, Laure Pisella <sup>1,5</sup> & Yves Rossetti <sup>1,2,5</sup>

The most striking pathological manifestation of spatial cognition is visuospatial neglect in which patients omit contralesional stimuli by failing to process important features on the left side of visual or mental scenes. Despite decades of extensive neuropsychological exploration, this syndrome has still not revealed all its mysteries. Here we present the case of a person with visuospatial neglect who spontaneously produced 40 paintings in the 3 years following his stroke. By analysing the spatial distribution of colour entropy in these paintings over the course of recovery we found that these paintings contain perturbations that include changes in colour use. This approach, borrowed from statistical physics and information theory, revealed left-right asymmetries in boundary line length of monochromatic patches as well as in colour components. While the unpainted canvas surface disappeared as soon as 26 weeks post-stroke, left-right colour patch asymmetries displayed a slower recovery over one hundred weeks. Several hypotheses that can be tested in future research emerged from this study, including the possibility that these phenomenological findings demonstrate several distinct recovery mechanisms at work.

Visuospatial neglect is classically defined as a lateralised attentional bias resulting in omissions in contralesional space, more common, severe and persistent following right cortical hemisphere damage<sup>1</sup>. However, visuospatial neglect is a polymorphic syndrome that cannot be explained by the sole attentional bias<sup>2,3</sup>. Depending on the delay<sup>4</sup> and the diverse location of the brain injury<sup>2-9</sup>, it can affect exploratory behaviour, action, perception and representation of both external and bodily spaces.

One approach to understanding visuospatial neglect involves administering a wide range of neuropsychological tests under highly controlled conditions, each of which efficiently sheds light on a specific aspect of the syndrome. These assessments are often complemented by evaluations of the patient's difficulties in performing daily activities. In addition to these quantitative approaches, the literature contains numerous compelling examples of artistic productions<sup>10-13</sup> which provide powerful visual insights

into the lived experience of visuospatial neglect. Their analysis, however, has typically been limited to anecdotal case reports, but when examined through the lens of narrative medicine, these artistic expressions offer a rich and underexplored source of knowledge. Narrative medicine, a growing field, enables patients and healthcare professionals to tell and listen to the complex and unique stories of illness using a variety of mediums.

Paintings, in particular, serve as a valuable medium within narrative medicine, where patients' spontaneous pictorial expressions convey essential information about their unique experiences with illness and recovery. Here, we exploit this rich source of information about intentional, perceptual and representational symptoms through quantitative analysis of a large series of artworks painted by patient F.B. in the three years following his right hemisphere stroke. Beyond established interacting factors involved in visual scene exploration —goal-directed and stimulus-driven actions, local

<sup>1</sup>Université Claude Bernard Lyon 1, CNRS, INSERM, Centre de Recherche en Neurosciences de Lyon CRNL U1028 UMR5292, TRAJECTOIRES, Bron, France.

<sup>2</sup>Service de Médecine Physique et Réadaptation, Plateforme Mouvement et Handicap, Hôpital Henry Gabrielle, Hospices Civils de Lyon, Saint Genis Laval, France.

<sup>3</sup>Laboratoire de Neuropsychologie Interventionnelle, Département d'Etudes Cognitives, ENS, PSL Research University, UPEC, Université Paris-Est, CNRS, Paris, France Paris-Est, CNRS, Paris, France. <sup>4</sup>Sorbonne Université, Sciences, normes, démocratie (SND), UMR 8011, 1 rue Victor Cousin, Paris, France. <sup>5</sup>These authors contributed equally: Laure Pisella, Yves Rossetti. <sup>6</sup>These authors jointly supervised this work: Gilles Rode, Eric Chabanat. e-mail: [gilles.rode@univ-lyon1.fr](mailto:gilles.rode@univ-lyon1.fr);

[gilles.rode@chu-lyon.fr](mailto:gilles.rode@chu-lyon.fr)

and global perception and representation of current frame selection —, each of which are crucial for understanding visuospatial neglect<sup>14–18</sup>, the paintings offer access to another, unsuspected dimension of visuospatial neglect: colour complexity asymmetry.

### Qualitative description of the artwork

We had access to dated paintings when F.B. exposed his work in an art gallery, well after they were completed. As a consequence, the natural or pictorial models were not available for comparison, and the artist explained that several paintings were produced without models. Nevertheless, the stark contrast in the amount of information (the complexity) between the left and right sides of the canvases, was striking from the observation of the paintings, reflecting differences in motor engagement and the way these areas are perceived and represented. The earliest paintings lacked paint on the left side of the canvas (e.g., Figure 1, week 8): this deficient behaviour is a typical feature of visuospatial neglect. Despite rapidly recovering the ability to cover the whole canvas surface, disappearance of these omissions did not mark the end of the recovery process, but rather the beginning of a long and slow process of reappropriation of left space. Indeed, F.B. produced large monochromatic dull areas on the left side of the canvas (e.g., Figure 1, week 32) and their colours and boundaries progressively increased in complexity over time (e.g., Figure 1, week 85). To quantify this complexity, we used entropy, a measure that captures both the amount of information in a signal and the regularity of its organization. We developed a method that incorporates colour components —Hue, Value, and Saturation— and entropy calculations, to assess left-right gradients of colorimetric information within each artwork and track how this complexity evolved over time.

## Methods

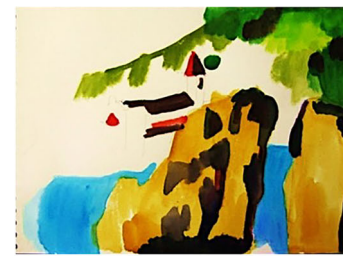
### F.B.'s story

F.B., a 58-year-old right-handed, male architect with a history of arterial hypertension was admitted to a neurological unit in August 2004 following the sudden onset of left hemiplegia and left visuospatial neglect without left homonymous hemianopia, consecutive to a deep, right hemispheric hematoma. Axial MRI found a right subcortical lesion affecting the insula and the putamen, and sparing the cortical attention<sup>4</sup> and colour processing networks<sup>19–21</sup> (Fig. 2A, B, D). Diffusion Tensor Imaging (DTI) analysis of white matter tract integrity found degradation in the inferior fronto-occipital fasciculus and the short fronto-insular tracts (Fig. 2C). He was transferred to our rehabilitation unit two months post-stroke, at which time he had persistent left-sided motor and somatosensory deficits associated with a sustained right-sided ocular and cephalic deviation and neuropsychological testing revealed left visuospatial neglect (see Supplementary Note 1). In addition to classical motor and cognitive rehabilitation, F.B. participated in art therapy sessions. Despite having never painted before, he enthusiastically took this up as a leisure activity. He spent several hours a day painting and produced a large number of paintings until June 2007 (Supplementary Fig. 1). Such intense, atypical engagement in a creative activity has already been described in other patients with lesions including the insula<sup>22,23</sup>. Neuropsychological assessment in April 2007 found complete regression of visuospatial neglect (Supplementary Note 1).

### F.B.'s paintings

We decided to analyse paintings containing landscape scenes painted between the 8th and 130th weeks following his stroke on canvases between 30 and 80 cm in width and 40 and 60 cm in height. Portraits and small formats were excluded for the sake of homogeneity. In accordance with national and institutional regulations ethical approval was not required for this study. Nevertheless, F.B. gave written consent authorising the authors to photograph, analyse and publish his paintings.

During the entire follow-up period, due to the patient's persistent hemiplegia, the painting easel and all the painting tools were positioned by his carer, such that the midpoint of the canvas was always in the same position relative to his wheel-chair. This allowed us to analyse the temporal evolution of the spatial asymmetries.



Week 8



Week 22



Week 32



Week 85



Week 114



Week 130

**Fig. 1** | Six sample canvases painted by F.B. at weeks 8, 22, 32, 85, 114, and 130 post stroke. All paintings can be found in Supplementary Fig. 1.

We hung each canvas on a wall and photographed it using the same field of view and under natural light. Each photograph was then displayed on a computer screen and divided into two equal sides by a line passing through the middle. Three parameters were measured for the left and right sides of each canvas, and analysed across

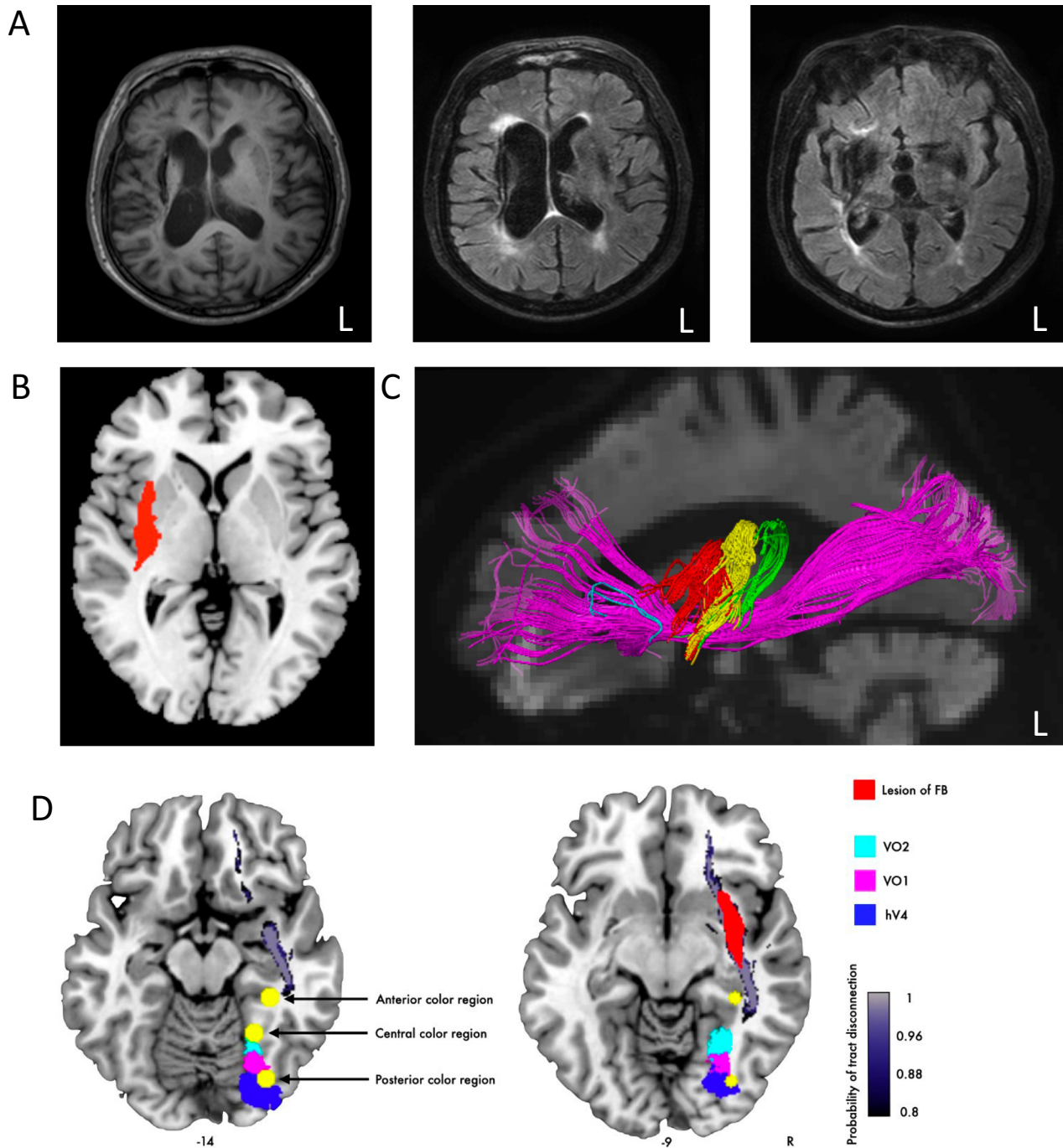


**Fig. 2 | Lesion analysis of patient F.B.** **A** Axial T1 and T2 MRI. **B** Reconstruction of patient’s brain lesion. **C** Reconstruction of the right damaged inferior Fronto-Occipital Fasciculus and the short Fronto-Insular Tracts. **D** Absence of overlap between FB’s lesion and colour processing networks. The lesion (in red) and white matter damage (defined by the probability of disconnection obtained by the

BCBtoolkit<sup>19</sup>) did not involve the anterior, central or posterior colour processing network<sup>20</sup> (yellow dots represent 5 mm spheres centered on the activity peaks of each region, here represented in the right hemisphere). The lesion also spared ventral colour regions hV4 (blue), VO1 (pink) or VO2 (cyan)<sup>21</sup>.

time: 1) unpainted surface area, 2) colour complexity along the horizontal axis, 3) monochromatic patch boundary length on each side of the canvas.

**Unpainted surface area**

For each canvas the unpainted surfaces were coloured in black on transparent paper (see Fig. 3, C1) then quantified using a Leica imaging system and Quantimet 500 software<sup>7</sup>. This value was then expressed as a percentage of the surface of area of the whole canvas.

**Colour complexity**

We studied the colour complexity of each painting using the HSV (Hue, Saturation, Value) human colour space model (Fig. 3)<sup>24</sup>. Hue is expressed as an angle between 0° (red) and 360° (purple), Saturation is expressed as a number on a linear scale between 0 (pale) and 1 (vivid), and Value of brightness is expressed as a number on a linear scale between 0 (black) and 1 (white). In statistical physics, entropy is a measure of the amount of disorder in a system, i.e., the more complex a system the greater its entropy. Shannon entropy comes from Information Theory and is related to the amount of

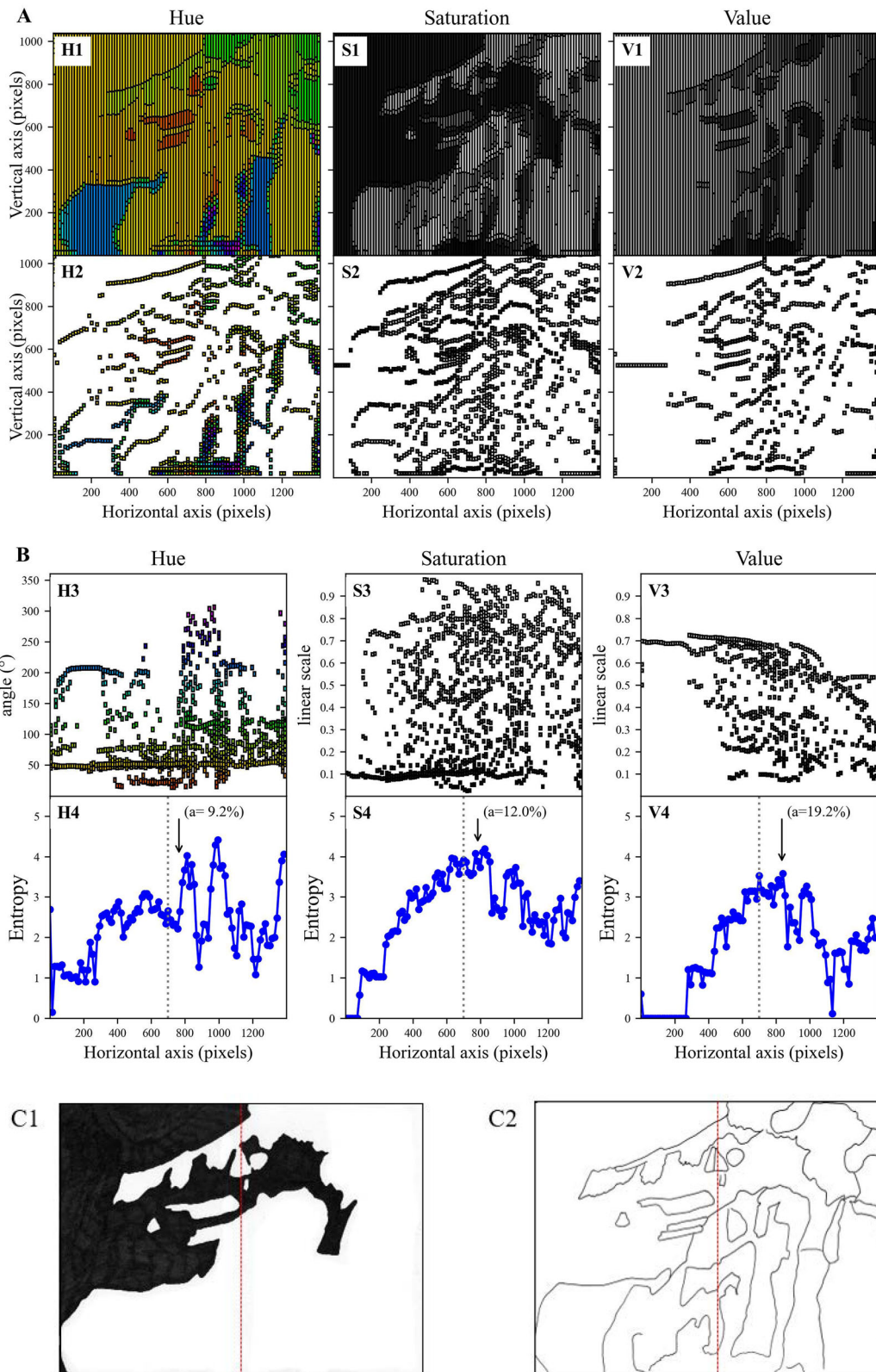


**Fig. 3 | Colour complexity of a painting made during week 12 using the HSV (Hue, Saturation, Value) human colour space model. A** XY decomposition of image pixels along the HSV dimensions. **B** Distribution along the horizontal axis of H, S, V components of the colour blobs (H3, S3, V3) and of the colour complexity (entropy) for each of the 100 columns (H4, S4, V4 where the vertical lines represent

the spatial center separating the left and right halves of the canvas and the black arrows represent the complexity barycenter (asymmetry index *a*)). **C** Unpainted surfaces (**C1**) and boundary lines separating patches of homogeneous colour (**C2**). See Supplementary Fig. 2 for the colour complexity of each of the 40 paintings.

information contained in a message. In order to carry out this calculation several steps were necessary. Using the definition of Shannon entropy<sup>25</sup> ( $H = -\sum_{i=1}^N p_i \log_2 p_i$ ) (1), painting complexity was computed separately for the H, S and V components of the colour decomposition (Fig. 3 H4, S4, V4). First, photographs of each canvas (in Portable Network Graphic (.png) file format) were H,S,V decomposed and divided into  $N = 100$  horizontal columns of equal width (Fig. 3A H1, S1, V1). A slope detection algorithm was then applied to the H, S, and V components separately to identify relatively uniform colour blobs. In Fig. 3A (H1, S1, V1) each blob is represented with a uniform colour component determined by the slope detection algorithm. Figure 3A (H2, S2, V2) shows the same colour blobs in a slightly different way: only the central point of each blob is represented (using the same colour component found in that blob). This XY representation makes it possible to visually observe the number of monochromatic blobs in each column and their HSV components (colour or greyscale of data points). Figure 3B (H3, S3, V3) illustrates these data in yet another way, showing the HSV distribution for each of the 100 columns along the horizontal axis only. Finally, Shannon entropy was computed with the probability  $p_i = \frac{\Delta y_i}{y}$  (2) where  $\Delta y_i$  is blob height and  $y$  column height. Since column height is always the same for a given painting, entropy values at different points along the horizontal axis are comparable with each other. Based on the spatial profiles of these colour components (Fig. 3B, H4, S4, V4), an entropy asymmetry index ( $a$  on Fig. 3B) was computed for each painting as the percentage of deviation from the spatial center of the canvas to the complexity barycenter along the horizontal axis.

These index values were then fitted as a function of recovery time. The best model required a plateau at the start of recovery (at value  $a_0$ , duration  $t_0$ ), followed by an exponential decrease (time constant  $\tau$ ) until the end of recovery.

$$a(t) = \begin{cases} a_0 & \text{for } t \leq t_0 \\ a_0 e^{-(t-t_0)/\tau} & \text{for } t > t_0 \end{cases} \quad (3)$$

The parameters  $t_0$ ,  $a_0$  and  $\tau$  were adjusted to reproduce the data as closely as possible. The calculation of asymmetry does not formally allow for the determination of its uncertainty. Moreover, since this quantity varies over time, a simple estimation of the standard deviation cannot be performed. To estimate a reliable value for the uncertainty in asymmetry, we used the standard deviation of the values obtained from the plateau, ensuring the consistency of the final fit. The procedure employed was as follows:

1. Calculate the standard deviation of the asymmetry values over the first  $n$  paintings.
2. Perform the fit using the above model.
3. Compute the residuals from this fit and iterate over  $n$  until residuals follow a standard normal distribution (mean value of 0 and standard deviation of 1).

In this case, if  $\chi^2/\text{df}$  (4) (goodness of fit  $\chi^2$  divided by the number of degrees of freedom) is close to 1, the fit between the data and the model is perfectly consistent. The model is therefore valid, and the standard deviation of its parameters (the values of  $a_0$ ,  $\tau$  and  $t_0$ ) is determined while accounting for the variability in the initial data. The width of the resulting 95% confidence intervals is thus not underestimated and accurately reflects the statistical precision derived from the data. A positive value of  $a_0$  with a confidence interval that does not include zero indicates significant deviation of the complexity barycenter to the right side of the painting.

### Patch boundary length

An art school teacher, naïve to the purpose of the study, was asked to draw lines along the boundaries separating patches of homogeneous colour with an Indian ink pen on transparent paper. The total length of these boundary lines was then measured for the right and left halves of each canvas using a curvimeter. Linear regressions of the temporal evolution of boundary line length were first performed separately for the left and right sides. The relevant comparison concerns the expected difference between left and right slopes of those temporal evolutions. This was interpreted based on the

significance of the regressions. A laterality index (LI) was then computed using the formula:  $(LI = (l_R - l_L)/(l_R + l_L))$ , (5) where  $l_L$  and  $l_R$  represent total line length for the left and right halves of the canvas. The evolution in time of the LI was fitted using a simple exponential model  $(LI(t) = a_0 e^{-\ln(2)t/T})$  (6) where  $a_0$  represents the estimated LI at time 0 and  $T$  the half-period of decrease (The laterality index decreases by half with each half-period). A positive value of  $a_0$  (and 95% confidence interval not including 0) indicates significantly longer total length of right-sided boundaries i.e., more detailed pictorial composition on the right half, either because patches have more complex shapes or because there are a greater number of patches.

For tests that assume a normal distribution data distribution was assumed to be normal but this was not formally tested.

### Reporting summary

Further information on research design is available in the Nature Portfolio Reporting Summary linked to this article.

### Results

#### Disappearance of unpainted surface area

More than 40% of the canvas was unpainted in the first artwork, this percentage decreased drastically already at week 10 but increased again in the following weeks. The temporal evolution of the percentage of unpainted area of the whole canvas is depicted in Fig. 4A and shows complete disappearance from the 26th week. This curve is superimposed on Fig. 4B, C as a grey area to contrast this rapid disappearance of omissions compared to the slow evolution of the other parameters.

#### Disappearance of colour asymmetry

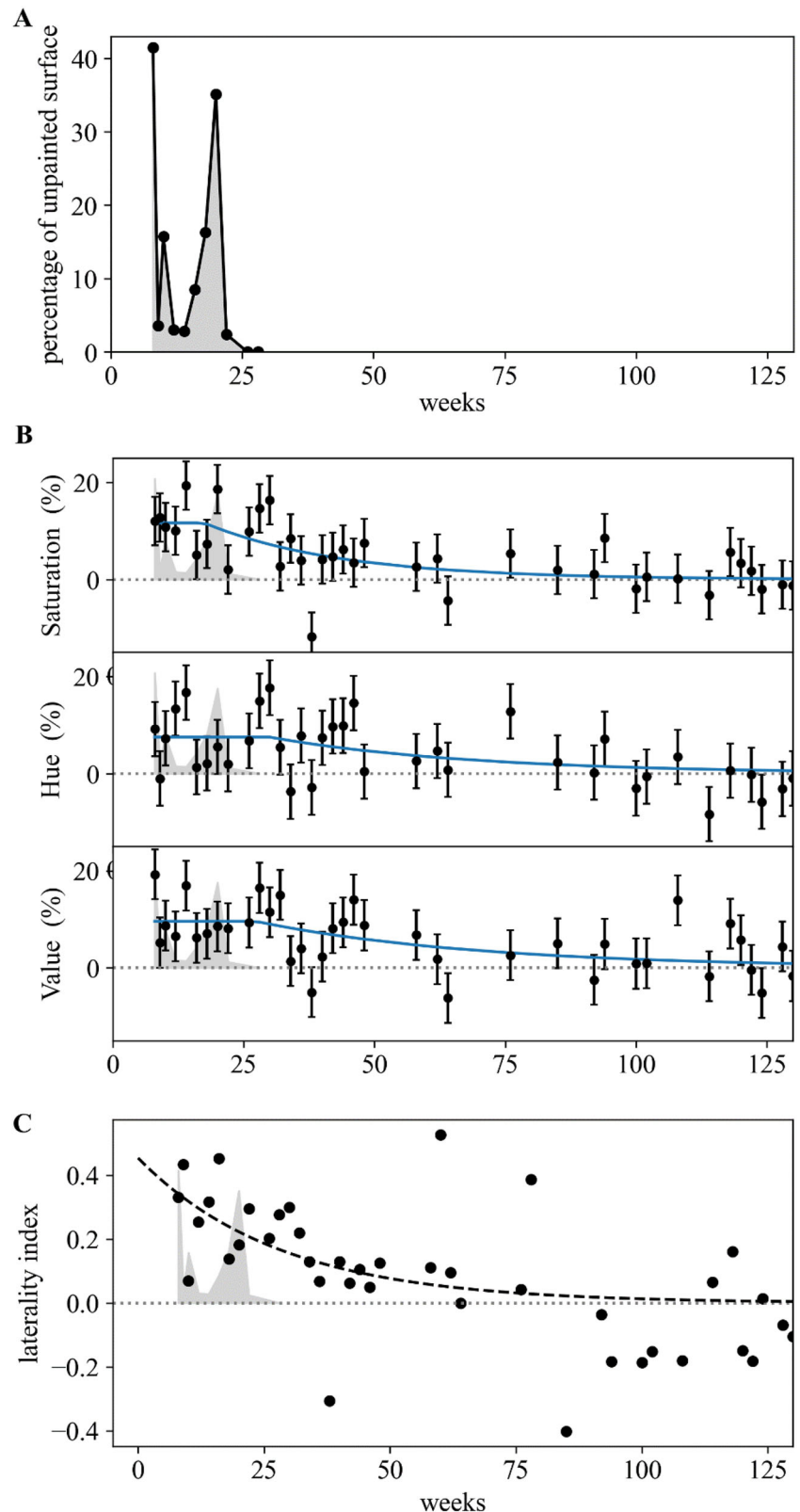
Direct observation of the paintings suggests a qualitative and quantitative asymmetry in colour choice. Qualitatively, the left-side colours appear colder (Hue more toward the blue), duller (less Saturation) and darker (less Value). For example, F.B. did not use the same shades of red and brown on both sides of the week 32 painting shown in Fig. 1. Quantitatively, a larger variety of colours on the right side of the paintings, observable in the three earliest paintings in Fig. 1, was measured by the rightward shift of the complexity barycenter (e.g. black arrows Fig. 3B). Barycenter values for each painting and each colour component are shown in Supp. Information 4 and are plotted as a function of time in weeks in Fig. 4B.

The follow-up analysis showed that the left-right entropy asymmetry in the three colour components (Hue, Saturation, Value) evolved with similar time courses. Each recovery curve consists of two phases: a positive plateau observed for each colour component around 10% with a confidence interval that did not include zero (7.5%,  $t(37) = 4.42, p < 0.0001, 95\text{CI} = [4.2, 10.8]$  for Hue, 11.7%,  $t(37) = 5.57, p < 0.0001, 95\text{CI} = [7.8, 15.6]$  for Saturation, and 9.6%,  $t(37) = 5.33, p < 0.0001, 95\text{CI} = [7.6, 11.6]$  for Value, Table 1) denoting larger variety of colours on the right side of the paintings (and lasting until  $t_0$  estimated at 17 weeks (SD = 8) for Saturation, 27 weeks (SD = 14) for Value and 30 weeks (SD = 17) for Hue, Table 1), followed by a slow progressive reduction of entropy asymmetry (Fig. 4B). Note that error bars in this figure do not reflect experimental uncertainties, but are calculated in such a way as to obtain residual distribution for H, S, V following a normal distribution with standard deviation equal to 1. They thus reflect the estimated statistical uncertainty of the colour entropy asymmetry.

#### Disappearance of patch asymmetry

When there were no longer unpainted surfaces on the left side of the canvases, F.B. began to paint large monochromatic areas on the left side (patches). We measured the length of the boundaries around monochromatic patches separately for the left and the right sides of each canvas and computed a laterality index for each canvas, plotted as a function of time on Fig. 4C. Tables 2 and 3 provide adjusted parameters and their confidence intervals, for the laterality index (expressed as a percentage) evolution, and for the evolution of boundary line lengths in the left and right halves of the paintings. The significant initial asymmetry (Fig. 4C)

**Fig. 4 | Temporal Evolution of pictorial and chromatic analyses.** **A** Percentage of unpainted canvas surface (omissions).his curve is super-imposed on the axes in **(B, C)** (grey area) to contrast the rapid disappearance of omissions compared to the slower evolution of other parameters. **B** Colour entropy asymmetry for Hue, Saturation and Value. Blue curves correspond to the fitted model whose adjusted parameters are provided in Table 1. They show significantly positive plateaus with  $a_0$  parameters whose 95% CIs do not include zero (Table 1) objectifying the asymmetry of colour entropy in the paintings. This plateau phase was followed by an exponential recovery phase that eventually reached zero asymmetry. Error bars: estimated statistical uncertainty of the colour entropy asymmetry. **C** Left/right asymmetry (Laterality Index) of total boundary line length. Dashed curve: asymptotic exponential model fitting data of asymmetry recovery.



is attested by a confidence interval for adjusted parameter  $a_0$  of the LI that did not include zero (Table 2). The LI progressively decreased, over-sized patches on the left being replaced by pictorial compositions of increasing complexity, reflected by a slow significant slope of increase in patch boundary length on the left side, but no significant change on the right side. Indeed, linear regressions revealed a significant increase in slope (1.2 mm

per week,  $t(38) = 5.3$ ,  $p < 0.0001$ ,  $95\text{CI} = [0.7, 1.6]$ ) for left-side boundary line lengths illustrating both a regression of unpainted surface area and a more detailed pictorial composition. There was no statistically significant evidence for a change in the slope for the right-side boundary line lengths (0.2 mm per week,  $t(38) = 1.2$ ,  $p = 0.24$ ,  $95\text{CI} = [-0.2, 0.7]$ ). (Fig. 5, Table 3).

**Table 1 | Adjusted parameters for colour complexity asymmetries over time. df=37**

Coef	value	std. dev.	Student t (p)	95% CI	$\chi^2/df$ (p)
Hue, $\tau$ (week)	39	29	1.34 (0.09)	[-18, 95]	1.05 (0.38)
Hue, $a_0$ (%)	7.5	1.7	4.42 (<0.0001)	[4.2, 10.8]	
Hue, $t_0$ (week)	30	17	1.76 (0.04)	[-3, 63]	
Sat, $\tau$ (week)	26	12	2.16 (0.02)	[2.5, 49]	1.05 (0.30)
Sat, $a_0$ (%)	11.7	2.1	5.57 (<0.0001)	[7.8, 15.6]	
Sat, $t_0$ (week)	17	8	2.12 (0.02)	[1, 34]	
Val, $\tau$ (week)	43	23	1.87 (0.04)	[-3, 89]	1.17 (0.23)
Val, $a_0$ (%)	9.6	1.8	5.33 (<0.0001)	[7.6, 11.6]	
Val, $t_0$ (week)	27	14	2.25 (0.01)	[0, 54]	

**Table 2 | Adjusted coefficients for the negative exponential evolution of the laterality index. df = 38**

Coef	value	std. dev.	student t	95% CI	p
Index, intercept $a_0$ (%)	31	8	4.0	[15, 46]	<0.001
Index, half-period T (week)	21	7.6	2.8	[6, 37]	0.003

**Table 3 | Adjusted coefficients for boundary line lengths in the left and right halves of the paintings. df = 38**

Coef	value	std. dev.	student t	95% CI	p
Left, intercept (mm)	120	16	7.4	[88, 154]	<0.0001
Left, slope (mm/week)	1.17	0.22	5.3	[0.73, 1.61]	<0.0001
Right, intercept (mm)	195	16	12.2	[163, 227]	<0.0001
Right, slope (mm/week)	0.26	0.21	1.2	[-0.2, 0.7]	0.24

**Discussion**

By their use of highly constrained visuo-graphical tasks, the very nature of classic neuropsychological tests of visuospatial neglect restricts the variety of perturbations they are able to uncover. Our study of 40 spontaneously-produced paintings, which differs radically from this approach, enabled us to reveal a previously unseen facet of visuospatial neglect’s complexity. This exceptional artwork offers insights into both the unique experience of a single patient and the potential mechanisms driving visuospatial neglect recovery.

Visuospatial neglect cannot be captured solely by left-sided omissions that recovered as early as week 26 post-onset. This remarkably swift and complete disappearance of unpainted areas is likely to be due to dissipation of the tonic oculomotor and head posture bias<sup>5</sup> and leftward motor hypokinesia<sup>6,7</sup> that have often been described in the acute phase of neglect. Using the original analysis of colour entropy borrowed from statistical physics and information theory, we demonstrated longer-lasting representational spatial asymmetries related to colour choice<sup>26</sup> and colour patch complexity. The plateau of spatial asymmetry in the colour complexity for all H, S, V components could reflect a stable lack of saliency for the left part of real visual scenes or mental images that F.B. intended to paint. Indeed, neural models of imagery postulate that mental representation involves the same network as visual perception<sup>27,28</sup>. This plateau was followed by a slow process of attentional rebalancing. Over-sized monochromatic patches within left space may reveal a misrepresentation that can be explained by a perceptual under-estimation of the size of some patches<sup>29,30</sup> that F.B. intended to match to right-sided patches (hyperschemata<sup>31</sup>), or by a more global, coarse, appreciation of the left part of the visual scene which includes

fewer local details<sup>18</sup>. One possible explanation of F.B.’s visuospatial neglect is therefore the consequence of his unilateral lesion in terms of decreased responses to<sup>5-7</sup> and decreased stimulus saliency in<sup>14-17</sup> the neglected hemi-field, as well as asymmetric mental representations of left and right space<sup>29-31</sup>.

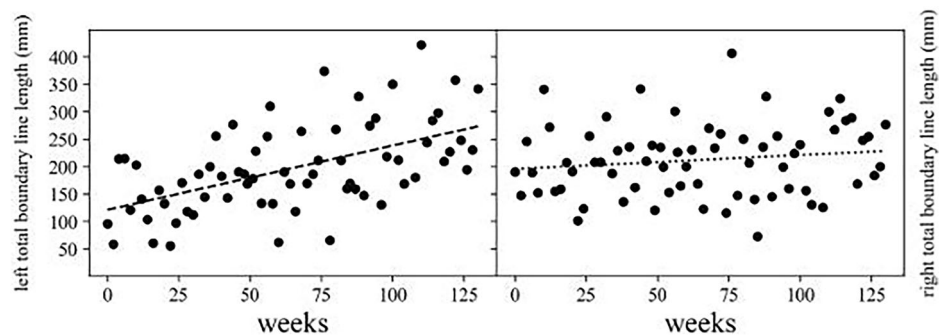
**Putative neurophysiological correlates of neglect and recovery in F.B**

The insula and the Fronto-Insular Tract (damaged in F.B.) have been put forward as a critical hub through which the ventral attentional network can “alert” and increase the activity of the dorsal attentional networks<sup>32</sup>. The evolution of F.B.’s artwork nicely depicts the behavioral and representational effects of the transient asymmetric activity and abnormal inter-hemispheric functional connectivity within the structurally-spared attention networks, that extends to motor and visual networks observed in similar cases of visuospatial neglect<sup>4,33</sup>. The asynchronous recovery of spatially oriented behaviour, followed by visual scene symmetry in object saliency and magnitude in the paintings, maps neatly onto distinct network normalization like that reported in the neuroimaging literature<sup>4,33</sup>. A previous study showed that almost complete visuospatial neglect behavioural recovery by 3 months post-stroke (measured with a neuropsychological battery) was significantly correlated with a normalization of inter-hemispheric functional connectivity across attention and sensorimotor networks, and a restoration of the normal anticorrelation between dorsal attention and motor regions<sup>33</sup>. Based upon the data of a neuroimaging study performed 4 weeks post-stroke following right insular lesion<sup>4</sup>, we speculate that the tonic endogenous orientation bias and the initial unpainted surfaces in F.B.’s artwork could be explained by the robust hyperactivation of parietal and sensorimotor cortex in the left, intact hemisphere at the acute stage. The longer-lasting representational asymmetries in the artwork could be explained by hypoactivation within spared visual regions in the right hemisphere, which is characteristic of the chronic stage evaluated at 39 weeks post-stroke in other patients<sup>4</sup>. Reduced visual response activity in the structurally intact primary and ventral occipital cortex<sup>4</sup> could explain the reduced variety of colours and appearance of less vivid colours on the left side of the canvases in F.B.’s paintings. The disruption of spatially selective responses in occipital-parietal cortices such that intact right visual cortex no longer responds preferentially to stimuli in the contralateral, left visual field has also been reported<sup>4</sup>, and could explain the spatial asymmetry in monochromatic patch size. The specific reactivation in the chronic phase of the retinotopic regions that code for the left visual field in the intact right dorsal visual cortex<sup>4</sup> could lead the *recalibration* of neural representation of left space within the structurally spared dorsal occipito-parietal cortex, involved in magnitude estimation of contralateral visual stimuli<sup>29,30</sup>.

**Future research on putative role of artistic endeavours in recovery**

This series of painting offer a visual narrative of patient FB’s visuospatial neglect recovery journey but *a posteriori* raise the question of whether the act of painting itself contributed to his recovery. Indeed, rehabilitation of visuospatial neglect relies on therapist-driven guidance and feedback which restricts a person’s capacity to autonomously foster a new relationship with space. In contrast, spontaneous painting involves free artistic expression. Moreover, the frame around the canvas offers a unique form of feedback revealing the disparity between intention to cover the whole canvas and the final, asymmetric outcome, thereby providing a concrete depiction of mental representations. The painting therefore projects the person into a new spatiality that contributes to recovery of action, attention and finally spatial symmetry. Using the words of Merleau-Ponty: “aesthetic perception in turn opens a new spatiality, and the painting as a work of art is no longer in the space that it inhabits as a physical thing or as a coloured canvas<sup>34</sup>. The painting is not only a representation of mental objects (memories or images of a landscape) or material objects (the landscape seen by the patient), it is also an intentionality, defined as a “*skilful bodily responsiveness*

**Fig. 5 | Total boundary line length for left and right-sides of each canvas.** Total length of boundary lines (in mm) drawn around monochromatic patches in the left and right halves of each canvas as a function of time from the first painting (8 weeks post-stroke). Linear regressions revealed a significant increase in slope (1.2 mm per week, 95% CI = [0.7, 1.6],  $p < 0.001$ ) for left-side boundary line lengths illustrating both a regression of unpainted surface area and a more detailed pictorial composition. There was no statistically significant evidence for a change in the slope for the right-side boundary line lengths (0.2 mm per week, 95%CI = [-0.2, 0.7],  $p = 0.24$ ).



and spontaneity in direct engagement with the world<sup>65</sup>, the perceiver is engaged in the world and what they can act upon depends on what they perceive.

### Limitations

We have proposed that the recovery of spatially oriented behaviour (measured by the evolution of parameters extracted from the paintings) may correlate with changes in brain activity, and that painting itself may play a beneficial role in visuospatial neglect recovery. However, these hypotheses remain speculative, as there is currently no experimental evidence to support them. Future research should test these hypotheses directly through prospective experimental protocols. For example, future research could include a series of single-case longitudinal studies that take multiple measures at numerous time points (e.g., functional recovery scales, functional neuroimaging with a Posner protocol, and analysis of spontaneously-produced paintings using the entropy approach developed in this paper) and specifically explore the correlations between these parameters. Given the significant variability in lesion sites associated with visuospatial neglect<sup>2–9</sup>, inclusion of a diverse group of patients with different lesion locations would enhance the value of this approach. Future research could also compare the time course of the functional recovery of two groups of hemineglect patients: one regularly engaging in colouring activities (e.g., mandalas or pre-designed line drawings) and the other regularly practicing spontaneous painting (with or without a model).

### Conclusion

Many aspects of visuospatial neglect remain elusive, but combining neuroimaging and functional investigations with narrative approaches could uncover new facets of this fascinating syndrome. This unique series of paintings, along with our analysis, has led to the formulation of several hypotheses. Humans represent their world in diverse ways, including through language and art. By designing experimental protocols that incorporate patients' discourse about their condition as well as analyses of their artistic expressions, we can gain deeper insights into each individual's unique experience. This pluralistic approach would not only enable patients to express themselves in their preferred mode, but could also offer access to previously-unexplored dimensions of the visuospatial neglect experience. The knowledge gained from this approach could then be used to generate new, testable hypotheses.

### Data availability

Digital copies of all 40 paintings are included in the SI. All datasets generated from the paintings can be found here: <https://osf.io/akczv/>.

### Code availability

All custom-made python code used to generate and analyse the datasets used in this paper can be found here: <https://osf.io/akczv/>.

Received: 14 March 2024; Accepted: 5 March 2025;

Published online: 26 March 2025

### References

1. Heilman, K. M., Watson, R. T. & Valenstein, E. Neglect and related disorders. in *Clinical Neuropsychology* (eds. Heilman, K. M. & Valenstein, E.) 296–346 (Oxford University Press, Oxford, 2003).
2. Halligan, P. W., Fink, G. R., Marshall, J. C. & Vallar, G. Spatial cognition: evidence from visual neglect. *Trends Cogn. Sci.* **7**, 125–133 (2003).
3. Rode, G., Pagliari, C., Huchon, L., Rossetti, Y. & Pisella, L. Semiology of neglect: An update. *Ann. Phys. Rehabil. Med.* **60**, 177–185 (2017).
4. Corbetta, M., Kincade, M. J., Lewis, C., Snyder, A. Z. & Sapir, A. Neural basis and recovery of spatial attention deficits in spatial neglect. *Nat. Neurosci.* **8**, 1603–1610 (2005).
5. Watson, R. T., Miller, B. D. & Heilman, K. M. Nonsensory neglect. *Ann. Neurol.* **3**, 505–508 (1978).
6. Heilman, K. M., Bowers, D., Coslett, H. B., Whelan, H. & Watson, R. T. Directional hypokinesia: prolonged reaction times for leftward movements in patients with right hemisphere lesions and neglect. *Neurology* **35**, 855–859 (1985).
7. Mattingley, J. B., Bradshaw, J. L. & Phillips, J. G. Impairments of movement initiation and execution in unilateral neglect. Directional hypokinesia and bradykinesia. *Brain* **115**, 1849–1874 (1992).
8. Verdon, V., Schwartz, S., Lovblad, K.-O., Hauert, C.-A. & Vuilleumier, P. Neuroanatomy of hemispatial neglect and its functional components: a study using voxel-based lesion-symptom mapping. *Brain* **133**, 880–894 (2010).
9. Takamura, Y., Fujii, S., Ohmatsu, S., Morioka, S. & Kawashima, N. Pathological structure of visuospatial neglect: A comprehensive multivariate analysis of spatial and non-spatial aspects. *iScience* **24**, 102316 (2021).
10. Halligan, P. W. & Marshall, J. C. Graphic neglect—more than the sum of the parts. *Neuroimage* **14**, S91–S97 (2001).
11. Halligan, P. W. & Marshall, J. C. The art of visual neglect. *Lancet* **350**, 139–140 (1997).
12. Blanke, O. & Pasqualini, I. The riddle of style changes in the visual arts after interference with the right brain. *Front Hum. Neurosci.* **5**, 154 (2011).
13. Cantagallo, A. & Della Sala, S. Preserved insight in an artist with extrapersonal spatial neglect. *Cortex* **34**, 163–189 (1998).
14. Karnath, H. O. & Niemeier, M. Task-dependent differences in the exploratory behaviour of patients with spatial neglect. *Neuropsychologia* **40**, 1577–1585 (2002).
15. Ptak, R., Golay, L., Müri, R. M. & Schneider, A. Looking left with left neglect: the role of spatial attention when active vision selects local image features for fixation. *Cortex* **45**, 1156–1166 (2009).
16. Bays, P. M., Singh-Curry, V., Gorgoraptis, N., Driver, J. & Husain, M. Integration of goal- and stimulus-related visual signals revealed by damage to human parietal cortex. *J. Neurosci.* **30**, 5968–5978 (2010).
17. Fellrath, J. & Ptak, R. The role of visual saliency for the allocation of attention: Evidence from spatial neglect and hemianopia. *Neuropsychologia* **73**, 70–81 (2015).

18. Marshall, J. C. & Halligan, P. W. Seeing the forest but only half the trees? *Nature* **373**, 521–523 (1995).
19. Foulon, C. et al. Advanced lesion symptom mapping analyses and implementation as BCBtoolkit. *Gigascience* **7**, 1–17 (2018).
20. Lafer-Sousa, R., Conway, B. R. & Kanwisher, N. G. Color-Biased Regions of the Ventral Visual Pathway Lie between Face- and Place-Selective Regions in Humans, as in Macaques. *J. Neurosci.* **36**, 1682–1697 (2016).
21. Wang, L., Mruczek, R. E. B., Arcaro, M. J. & Kastner, S. Probabilistic Maps of Visual Topography in Human Cortex. *Cereb. Cortex* **25**, 3911–3931 (2015).
22. Thomas-Anterion, C. et al. De novo artistic activity following insular-SII ischemia. *Pain* **150**, 121–127 (2010).
23. Camenzind, M., Eberhard-Moscicka, A. K., Cazzoli, D. & Müri, R. M. Hyperzographia in Neglect Exposing a Spatial Dissociation between Painting and Writing—A Case Study. *Reports* **5**, 32 (2022).
24. Smith, A. R. Color gamut transform pairs. *SIGGRAPH Comput. Graph.* **12**, 12–19 (1978).
25. Shannon, C. E. A Mathematical Theory of Communication. *Bell Syst. Tech. J.* **27**, 379–423 (1948).
26. Vatanparasti, S., Kazemnejad, A. & Oveisgharan, S. Non-invasive Brain Stimulation and Prism Adaptation in Art Constructive Errors in Painting. *Basic Clin. Neurosci.* **14**, 143–154 (2023).
27. Kosslyn, S. M. *Image and Brain The Resolution of the Imagery Debate*. (MIT Press, Cambridge, MA, 1996).
28. Bartolomeo, P. The relationship between visual perception and visual mental imagery: a reappraisal of the neuropsychological evidence. *Cortex* **38**, 357–378 (2002).
29. Cohen, L., Gray, F., Meyrignac, C., Dehaene, S. & Degos, J. D. Selective deficit of visual size perception: two cases of hemimicropsia. *J. Neurol. Neurosurg. Psychiatry* **57**, 73–78 (1994).
30. Jurkiewicz, T., Salemme, R., Froment, C. & Pisella, L. Role of the Dorsal Posterior Parietal Cortex in the Accurate Perception of Object Magnitude in Peripheral Vision. *Iperception*, <https://doi.org/10.1177/20416695211058476> (2021).
31. Rode, G., Michel, C., Rossetti, Y., Boisson, D. & Vallar, G. Left size distortion (hyperschematia) after right brain damage. *Neurology* **67**, 1801–1808 (2006).
32. Menon, V. & Uddin, L. Q. Saliency, switching, attention and control: a network model of insula function. *Brain Struct. Funct.* **214**, 655–667 (2010).
33. Ramsey, L. E. et al. Normalization of network connectivity in hemispatial neglect recovery. *Ann. Neurol.* **80**, 127–141 (2016).
34. Merleau-Ponty, M. *Phenomenology of Perception (Originally Published as Phénoménologie de La Perception (Gallimard, Paris, 1945))*. (Routledge, London, 2012).
35. Carman, T. *Merleau-Ponty*. (Routledge, London, 2012).

## Acknowledgements

We wish to thank F.B. for authorizing us to use his paintings in this study, Françoise Eiberlé and Philippe Sénéchal for their essential roles in initiating the project, Marcel Rode for his expertise and help in several steps of the analyses and Philip Robinson. The authors received no specific funding for

this work, but the Hospices Civils de Lyon, INSERM, CNRS and University of Lyon supported this work via staff salaries. The funders had no role in study design, data collection and analysis, decision to publish or preparation of the manuscript.

## Author contributions

G.R., L.P. and Y.R. conceived the idea, the study design and wrote the paper. E.C. and P.R. designed the model and the computational framework and analyzed the data. M.L. designed the methodology for analyzing brain MRI and tractography data. J.C. contributed to the analyses and the interpretation of results. K.R. contributed to the final version of the manuscript.

## Competing interests

The authors declare no competing interests.

## Additional information

**Supplementary information** The online version contains supplementary material available at

<https://doi.org/10.1038/s44271-025-00226-5>.

**Correspondence** and requests for materials should be addressed to Gilles Rode.

**Peer review information** *Communications Psychology* thanks Radek Ptak, Rene Müri and Margaret Jane Moore for their contribution to the peer review of this work. Primary Handling Editor: Marike Schiffer. A peer review file is available.

**Reprints and permissions information** is available at

<http://www.nature.com/reprints>

**Publisher's note** Springer Nature remains neutral with regard to jurisdictional claims in published maps and institutional affiliations.

**Open Access** This article is licensed under a Creative Commons Attribution-NonCommercial-NoDerivatives 4.0 International License, which permits any non-commercial use, sharing, distribution and reproduction in any medium or format, as long as you give appropriate credit to the original author(s) and the source, provide a link to the Creative Commons licence, and indicate if you modified the licensed material. You do not have permission under this licence to share adapted material derived from this article or parts of it. The images or other third party material in this article are included in the article's Creative Commons licence, unless indicated otherwise in a credit line to the material. If material is not included in the article's Creative Commons licence and your intended use is not permitted by statutory regulation or exceeds the permitted use, you will need to obtain permission directly from the copyright holder. To view a copy of this licence, visit <http://creativecommons.org/licenses/by-nc-nd/4.0/>.

© The Author(s) 2025